Chemistry of Heterocyclic Compounds, Vol. 50, No. 3, June, 2014 (Russian Original Vol. 50, No. 3, March, 2014)

5-[4-(*N*,*N*-DIMETHYLAMINO)PHENYL]-2-(4-PYRIDYL)-1,3-OXAZOLE AS A FLUORESCENT PROBE FOR MONITORING MICROHETEROGENEOUS MEDIA

O. O. Borodin[1], R. Yu. Il'yashenko[1], and A. O. Doroshenko[1]*

The N,N-dimethylamino-γ-pyridine analog of 2,5-diaryl-1,3-oxazole has been synthesized. Quantum-chemical modeling was carried out for the electronic absorption spectra and the effect of hydrogen bonding between the pyridine nitrogen atom and the water molecule on these spectra. The calculation results were compared with the experimental data for the solvent effect on the spectra of this compound. The feasibility of practical application of this derivative as a fluorescent probe was tested for determining the critical micelle concentration in aqueous solutions of nonionic, zwitterionic, cationic, and anionic surfactants.

Keywords: 2,5-diaryl-1,3-oxazole derivatives, Bader's AIM theory, critical micelle concentration, ESS analysis of electronic excitations, fluorescent probe, quantum-chemical calculations, solvatochromism.

Fluorescent organic compounds, whose spectral characteristics are a function of both general and specific intermolecular interactions with the solvent, have been used for many decades for probing microheterogeneous media such as colloidal solutions, microemulsions, and biological systems [1-4]. Most fluorescent probes are soluble to some extent in both water and lipophilic media and demonstrate a significant increase in the fluorescence quantum yield and/or change in fluorescent color upon entering the hydrophobic environment of surfactant micelles, cell membranes, protein globules, etc. [3, 4].

2,5-diaryloxazole derivatives are known to be efficient organic luminophores in the violet-blue spectral range [5], but the fluorescent characteristics of most of these compounds are not highly dependent on their microenvironment. Thus, their major application has been as liquid and plastic scintillation materials from the mid-twentieth century until now [6, 7]. In the present work, we have discovered a 2,5-diaryloxazole derivative serving as an efficient fluorescent probe and carried out a quantum-chemical analysis of its spectral and physicochemical properties. This compound was also tested in microheterogeneous systems consisting of aqueous colloidal solutions of various surfactants.

In order to make the 2,5-diaryloxazole derivative sensitive to the polar characteristics of the microenvironment, its chemical structure was modified to provide considerable redistribution of electron density in the electronically excited state: the benzene ring at position 2 was replaced by an electron-withdrawing

*To whom correspondence should be addressed, e-mail: andrey.o.doroshenko@univer.kharkov.ua, andrey.o.doroshenko@gmail.com.

[1]V. N. Karazin Kharkiv National University, 4 Svobody Sq., 61022 Kharkiv, Ukraine.

Translated from Khimiya Geterotsiklicheskikh Soedinenii, No. 3, pp. 413-423, March, 2014. Original article submitted January 29, 2014.

pyridine cycle, which provides for greater solubility of the resultant compound (the log *P* index calculated using an additive scheme was 2.97 for the pyridine derivative, while it was 4.23 for the benzene analog), and a dimethylamino group, which is a strong electron donor, was introduced in the benzene ring at position 5 of the oxazole moiety. In order to achieve the greatest spectral effects in accord with our previous recommendations [8], this molecule was constructed such that the direction of the redistribution of electron density between the introduced electron-donating and electron-withdrawing sites corresponded to the direction of the shift in electron density upon going to the excited state in the unsubstituted 2,5-diphenyloxazole molecule. 5-[4-(*N*,*N*-Dimethylamino)phenyl]-2-(4-pyridyl)-1,3-oxazole (**1**), which was synthesized in accord with this principle, was not found in the SciFinder [9] and Reaxys databases [10].

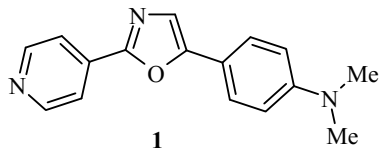

1

The structure of oxazole **1,** its spectral characteristics, and its intermolecular interactions with proton donors such as water were initially modeled using quantum-chemical approach by DFT methods, B3LYP/ cc-pVDZ calculation [11, 12] (TDDFT calculation for the excited molecules), the Bader's AIM theory [13-15], and ESSA (excited state structural analysis) [16]. ESSA is an approach for estimating the participation of individual atoms in electronic excitation and analyzing the redistribution of electron density in a molecule related to its transition to an electronically excited state.

Fluorescent probe **1** should display sensitivity to proton-donating compounds since this molecule has several nucleophilic sites, which are potential hydrogen bond acceptor sites, in addition to the polarity of the microenvironment. Our calculations showed strong intermolecular hydrogen bonding between the pyridine nitrogen atom in oxazole **1** and a water molecule; the calculated H···N bond length in the ground state was 1.97 Å. The hydrogen bond markedly contracts to 1.89 Å upon going to the lowest singlet ground state, which indicates that it becomes stronger.

The energy of the above-mentioned hydrogen bond was calculated using the AIM theory and semiempirical Espinosa approximation [17] based on an analysis of the electron density at its critical point {3, -1} ($\Delta E_{HB} \sim$ ½VIR, Virial Field Function). According to our calculations, the energy of the hydrogen bond formed by a water molecule with the pyridine nitrogen atom in oxazole **1** is enhanced by almost 25% in going to the electronically excited state: from 5.9 (S_0) to 7.3 kcal/mol (S_1).

The effect of the hydrogen bond with proton-donating molecules on the electronic spectra was analyzed for oxazole **1** using the ESSA approach [16], which presupposes calculation of special quantum-chemical indices, namely electron excitation localization numbers (L_i, %), which characterize the participation of individual atoms or submolecular fragments in the formation of a specific electronic transition, and the charge transfer numbers (l_{ij}, in % of electron charge), which give detailed picture of the redistribution of electron density upon transition of the molecule to the excited state [18]. In order to make this analysis more meaningful and avoid unnecessary details, the molecule of oxazole **1** was divided into four submolecular fragments, namely, the pyridine, oxazole, and benzene rings and the dimethylamino group, for which the electronic excitation localization numbers and charge transfer numbers were summed over all their atoms. The water molecule acted as an additional fragment for the hydrogen-bonded complex oxazole **1**···H_2O. However, as expected, no significant localization of electronic excitation was found on the atoms of the water molecule. Similarly, by the way, no displacement of electron density to the water molecule from the fragments of the major chromophore of oxazole **1** was found. Thus, the water molecule in the hydrogen-bonded complex acts only as a perturbing factor, which does not fundamentally alter the nature of the electronic transitions (Table 1).

The formation of the hydrogen-bonded complex with the water molecule at the pyridine nitrogen atom does not lead to a change in the nature of the electronic excitation localization relative to the free molecule of oxazole **1**. Only a slight increase was noted for the participation of the pyridine ring in the formation of the S_0–S_1 electron transition. On the other hand, the hydrogen bond leads to a somewhat greater redistribution of electron density in the molecule (see the charge transfer numbers l_{ij} and total charge changes on the selected submolecular fragments) in going to its lowest singlet excited state responsible for subsequent fluorescence emission. The vector difference of the dipole moments in the ground and excited states, which is a generally accepted quantitative index, also indicates greater electron density redistribution. The vector Δμ virtually coincides in its direction in space with the axis traversing the pyridine ring and dimethylamino group nitrogen atoms, which are the electron-withdrawing and electron-donating sites of oxazole **1**. The rather large value of Δμ would lead us to expect significant solvatofluorochromism (change in the position of the emission band upon change in the polarity of the surrounding medium) for the molecule studied. Furthermore, the above-mentioned enhanced nucleophilicity of the pyridine ring nitrogen in oxazole **1** in the electronically excited state should lead to an additional shift of the fluorescence band toward longer wavelengths in the presence of proton-donating molecules such as hydrogen bond donor solvents and traces of moisture in aprotic media.

TABLE 1. ESS Analysis of the Long-Wavelength Transitions in the Calculated Electronic Absorption Spectra of Oxazole **1** and Its H-Complex at the Pyridine Nitrogen Atom with a Water Molecule*

S_0–S_1 transition	Localization of electronic excitation	Electron density redistribution upon transition to the excited state
381 nm 26220 cm^{-1} f = 0.713	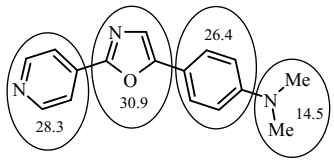	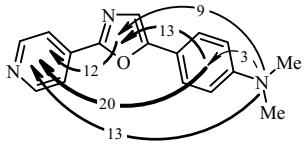 -0.444 -0.105 +0.304 +0.245 Δμ = 21.5 D
394 nm 25370 cm^{-1} f = 0.693	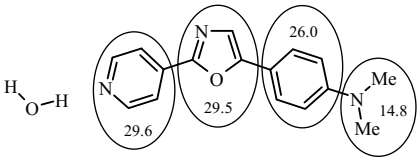	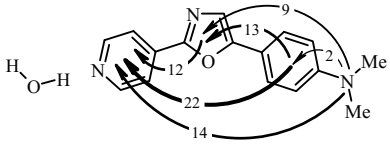 -0.478 -0.103 +0.325 +0.256 Δμ = 22.6 D

*This table gives the calculated characteristics for the long-wavelength electronic transition in the absorption spectra of oxazole **1** and its H-complex with a water molecule (position in terms of wavelength and wavenumbers, oscillator strength), localization of the electronic excitation in the structurally isolated submolecular fragments (L_i, % [16, 18]), and redistribution of electron density upon transition to the excited state (the numbers in the arrows give the charge transfer numbers (l_{ij} [16, 18]). The total change in electric charge on the selected submolecular fragments and the vector difference in the dipole moments in the molecule of oxazole **1** in the ground and excited states (D) are shown below the molecular diagrams.

TABLE 2. Spectral and Fluorescent Properties of 5-[4-(*N*,*N*-Dimethylamino)phenyl]-2-(4-pyridyl)-1,3-oxazole in Various Solvents*

Solvent	E_T^N	λ_a, nm	ν_a, cm^{-1}	λ_f, nm	ν_f, cm^{-1}	$\Delta\nu_{ST}$, cm^{-1}	φ_f
Hexane	0.009	343	29160	412	24280	4880	0.47
Toluene	0.099	347	28820	422	23700	5120	0.52
Dioxane	0.164	348	28740	446	22420	6320	0.44
Ethyl acetate	0.228	349	28660	456	21920	6740	0.41
1,2-Dichloroethane	0.327	350	28580	458	21840	6740	0.46
Dimethyl formamide	0.386	352	28400	547	18280	10120	0.18
Acetonitrile	0.460	354	28240	542	18460	9780	0.22
Ethanol	0.654	355	28160	552	18120	10040	0.17
Water	1.000	357	28020	542	18460	9560	0.03

*λ_a, λ_f, ν_a, ν_f are the positions of the absorption and fluorescence bands in terms of wavelength and wavenumbers, $\Delta\nu_{ST}$ is the Stokes shift, and φ_f is the fluorescence quantum yield. The polar properties of the solvent are characterized qualitatively by the empirical Reichardt parameter E_T^N [22].

Very often a strong intramolecular charge transfer in the electronically excited state of organic molecules results in quenching of their fluorescence in polar media [19-21]. Thus, a substantial increase in fluorescence intensity at transition from the proton-donating polar aqueous medium to environment of low polarity within the micelles, cell membranes, or protein globules, can be expected for compound **1**.

Our theoretical analysis indicates that oxazole **1** satisfies the major set of requirements for a fluorescence probe, namely, that it should display sensitivity to general and specific intermolecular interactions by reacting to change in its immediate microenvironment by change in both the color and intensity of the emitted fluorescence.

The spectral characteristics of oxazole **1** determined experimentally in a series of solvents differing in polarity and proton-donating capacity (Table 2, Fig. 1, the data given in Fig. 1 are only for aprotic solvents), on the whole, support our theoretical conclusions. The data obtained indicate that oxazole **1** does not show significant solvatochromism, while its solvatofluorochromism is rather pronounced. The fluorescence Stokes shift almost doubles in going from hexane to dimethyl formamide. High solvent polarity leads to a reduction in the fluorescence quantum yield, especially pronounced for aqueous solutions, in which the rather strong fluorescence of oxazole **1** found in nonpolar media is almost entirely quenched. Such a sharp change in the spectral parameters of a fluorescent probe relative to the polar and proton-donating characteristics of its closest molecular environment make it promising for fluorescent probing of microheterogeneous aqueous systems such as micelles and biological media.

Since the acidity of the medium under conditions for the possible use of oxazole **1** as a probe may vary in a rather broad range, it was also necessary to test this compound for sensitivity to pH. The results of the spectrophotometric acid-base titration are shown in Figure 2.

In the first stage of protolytic interactions, a marked shift of the absorption spectrum toward longer wavelengths is noted with a 30-35% drop in fluorescence intensity. This finding corresponds to protonation of the pyridine nitrogen atom in oxazole **1**, such that the intramolecular donor-acceptor interaction (charge transfer upon excitation) is enhanced substantially. The latter circumstance is most likely to be the cause of a drop in the fluorescence quantum yield of the monocation.

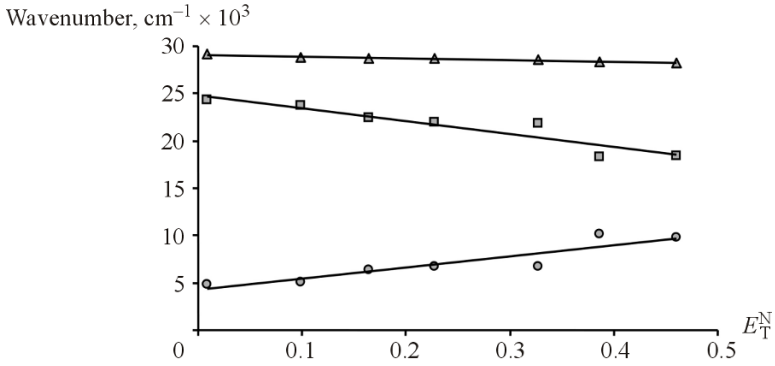

Fig. 1. Dependence of the position (from the top down) of the absorption spectrum, fluorescence spectrum, and fluorescence Stokes shift of oxazole **1** on the Reichardt polarity (E_T^N) of a series of aprotic solvents.

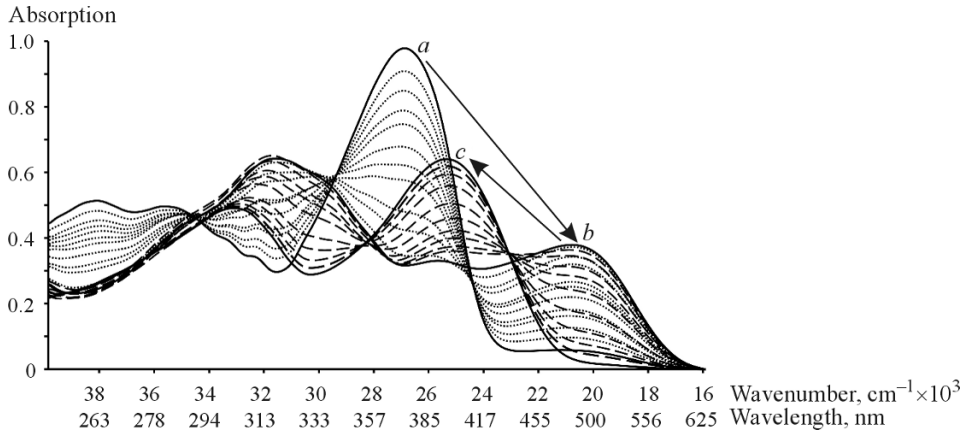

Fig. 2. Spectrophotometric acid-base titration of oxazole **1** at pH from 7 to 0.5, changes in the absorption spectrum with decreasing pH are shown by arrows: *a*) initial spectrum of the neutral form, *b*) spectrum at intermediate pH values ~3 with a maximal contribution of the monocationic form, and *c*) spectrum of the final solution with a high contribution of the dicationic form.

Further decrease in pH leads to a sharp shift of the absorption and fluorescence spectra toward shorter wavelengths due to the exclusion of the lone electron pair of the dimethylamino group nitrogen atom from the conjugation chain. The titration curves show two inflection points, corresponding to two stages of proton addition upon increasing acidity of the medium. Mathematical treatment of these curves permits evaluation of the equilibrium constants of the discussed protolytic reactions.

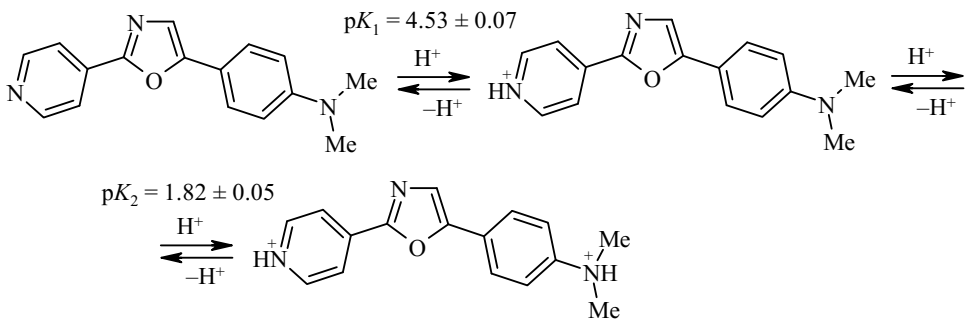

The basicity of the oxazole ring nitrogen atom is lower than for the pyridine nitrogen atom. Thus, the third protonation stage should be observed for a more acidic medium at pH < 0 (in the region described by acidity functions similar to the Hammett H_0 function). Thus, this fluorophore will be in its neutral form in the physiological pH range characteristic for most microheterogeneous biological systems.

The testing of oxazole **1** as a fluorescence probe for microheterogeneous media was carried out by evaluating the critical micelle concentrations (CMC) for aqueous solutions of several surfactants of different nature. Various methods are usually employed for determining this important colloid system index such as conductometry, surface tension measurements, spectrophotometry, etc. [23, 24].

A significant bathochromic shift of ~2000 cm^{-1} was observed in the absorption spectra upon the titration of aqueous solutions of oxazole **1** using the nonionic surfactant Brij-35 (lauryl ether of polyoxyethylene-23), while the fluorescence intensity increases by more than an order of magnitude, which is also accompanied by a slight shift of the emission band toward shorter wavelengths. These findings may be attributed to solubilization of oxazole **1** by surfactant micelles into their nonpolar near-surface zone.

The changes in the absorption spectra for zwitterionic surfactant, cetyl dimethylammonium propanesulfonate (CDAPS, the titration is presented as an example in Fig. 3) were similar to those for the nonionic surfactant but a marked shift toward longer wavelengths was observed in the fluorescence spectra. This result indicates greater polarity of the binding zone of oxazole **1** in the zwitterionic surfactant micelles.

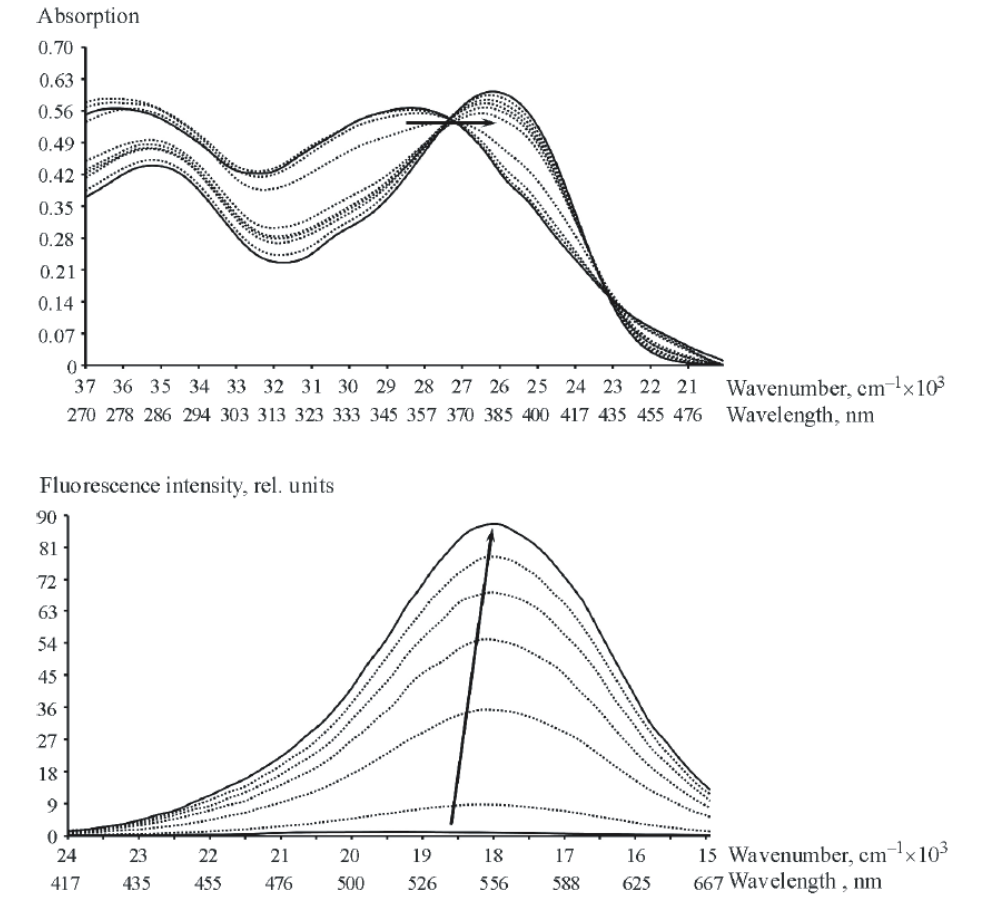

Fig. 3. Spectrophotometric and fluorimetric titration of oxazole **1** in an aqueous solution of the zwitterionic surfactant, CDAPS (concentration from 0 to $2 \cdot 10^{-3}$ M). The changes in the spectra upon increasing the surfactant concentration are indicated by arrows.

The greatest enhancement of the fluorescence of oxazole **1** by a factor of more than 50 was found for solutions of the cationic surfactant, cetyl trimethylammonium bromide (CTAB). A significant shift of the fluorescence band toward shorter wavelengths of about 1000 cm^{-1} was also observed. This finding is apparently a result of specific solvation of rather nucleophilic oxazole **1** by CTAB cations such that this probe enters the binding zone within the micelle with higher effective polarity than that for nonionic and zwitterionic surfactants.

Spectral changes fundamentally different from all the other cases examined were found for solutions of the anionic surfactant, sodium dodecyl sulfate (SDS). Absorption bands for the mono- and dication appeared in the absorption spectrum of oxazole **1** even before reaching the critical micelle concentration (Fig. 4), while the

TABLE 3. Monitoring of Various Microheterogeneous Micellar Media Using 5-[4-(*N*,*N*-Dimethylamino)phenyl]-2-(4-pyridyl)-1,3-oxazole as the Fluorescent Probe

Surfactant		λ_f, ($C_{surfactant}$ > CMC)	Increase in the fluorescence intensity by a factor of	CMC, M
Brij-35	nonionic	545	21	$6.7\cdot10^{-5}$ ($6.2\cdot10^{-5}$ [27])
CDAPS	zwitter-ionic	556	10	$3.6\cdot10^{-3}$ ($4.0\cdot10^{-3}$ [28])
CTAB	cationic	562	51	$9.8\cdot10^{-4}$ ($9.2\cdot10^{-4}$ [29])
SDS, pH 9.18	anionic	526	7	$8.8\cdot10^{-3}$ ($8.3\cdot10^{-3}$ [29])
SDPS	anionic	469	5	$8.6\cdot10^{-3}$ ($8.0\cdot10^{-3}$ [29])

absorption intensity of the monoprotonated form began to decrease above the CMC along with an increase in the absorption in the range characteristic for the dicationic form of oxazole **1**. The estimated value of the CMC of SDS ($9.4\cdot10^{-3}$ M) under these conditions was obtained with an unsuitably high systematic deviation from the literature data (Table 3).

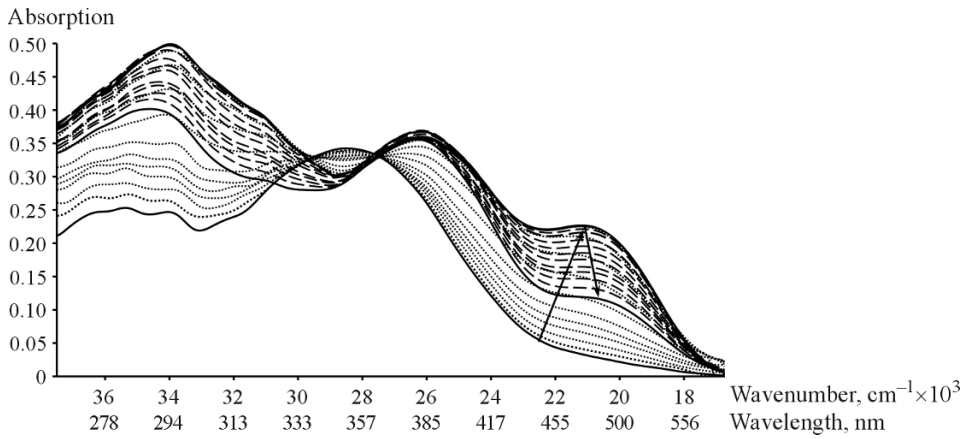

Fig. 4. Spectrophotometric titration of oxazole **1** in an unbuffered aqueous solution by the anionic surfactant, SDS (from 0 to $1.2\cdot10^{-2}$ M, the surfactant concentration below the CMC is indicated by dotted lines, while the surfactant concentration above the CMC is indicated by dashed lines). The changes in the spectra with increasing surfactant concentration are indicated by arrows.

The most characteristic difference between SDS micelles from other types of surfactants is their high surface density of negative charge [25, 26]. This increases the near-surface concentration of Na^+ and H^+ counterions, and consequently a substantial reduction of the local pH in the Stern layer, and thus to its

"acidification" compared with the intermicellar aqueous phase. Probe **1**, falling on the surface of the micelles SDS, undergoes protonation at the pyridine atom and stays there, without penetrating the hydrophobic regions in the depth of the micelle. Therefore, in this experiment the enhancement of its fluorescence was not observed. After achieving CMC, upon further increase in SDS concentration, acidity of the surface electrical double layer of micelles decreases so much that the equilibrium monocation-dication increasingly shifts to the latter. Since the probability of penetration of the dication form **1** to the interior of the micelles is even smaller than that of the discussed above monocation it further does not increase the intensity of the fluorescence of the probe associated with SDS micelles.

In order to check our conclusions concerning the reasons for the atypical behavior of oxazole **1** in solutions of an anionic surfactant, this compound was titrated with another anionic surfactant, not providing such high surface density of micellar negative charge as in the case of SDS, namely sodium dodecylphenylsulfonate (SDPS). In the latter case, protonation of oxazole **1** on the micelle surface does not occur and its fluorescence is enhanced upon solubilization though not to the same great extent as observed for micelles of nonionic, zwitterionic, and cationic surfactants.

The SDS titration of oxazole **1** in alkaline buffer solution at pH 9.18 under conditions such that the acidity of the micelle surface and the intermicellar aqueous phase differ only slightly leads to similar results. The cationic forms of oxazole **1** were not appeared in this case. Thus, the neutral probe molecules are solubilized within the micelles, which accompanied by a general increase in the fluorescence intensity. Under the conditions for the measurements in the buffer system, our experimental value for the critical micelle concentration of the anionic surfactant, SDS, proved much closer to the literature value than in the previous case, in which this index was tried to estimate without buffer.

The experimental data on the titration of aqueous solutions of oxazole **1** by various surfactants were mathematically treated to find the critical micelle concentration. Our quantitative results show rather satisfactory agreement (deviations not exceeding 10%) with the literature data for the various surfactants obtained by other methods [27-29] (Table 3).

Thus, we have synthesized a new 2,5-diaryloxazole fluorescent probe, namely, 5-[4-(*N*,*N*-dimethyl-amino)phenyl]-2-(4-pyridyl)-1,3-oxazole, which was subjected to experimental testing and theoretical analysis. This probe demonstrated its suitability for the quantitative monitoring of the physicochemical characteristics of microheterogeneous colloidal systems.

EXPERIMENTAL

^{1}H and ^{13}C NMR spectra (DEPT-135) were recorded on a Varian Mercury VX-500 spectrometer (500 and 125 MHz, respectively) in DMSO-d_6 with TMS as internal standard. Absorption spectra were recorded on a Hitachi U3210 spectrophotometer, and fluorescence quantum yields were registered on a Hitachi F4010 spectrofluorimeter. Quinine bisulfate in 0.5 M aqueous sulfuric acid (φ_f 0.546 [30]) was used as the standard for measuring the quantum yields.

The protolytic reaction constants of oxazole **1** were determined by treating the data of the spectrophotometric titration in 1:1 water–ethanol. pH of the water–ethanol solutions were measured using the EV-74 universal ion meter calibrated relative to standard aqueous buffer solutions with a correction of 0.02 pH unit [31].

In order to perform the titration using surfactant solutions, a solution of ~$2\cdot10^{-5}$ mol/l oxazole **1** was prepared with the same content and concentration of the surfactant thrice greater than the CMC. The titration was carried out in a standard 1-cm fluorimetric cell containing 2 ml initial aqueous solution of oxazole **1** and from 0.005 to 0.2 ml surfactant solution added by previously calibrated dosing apparatus. The absorption and fluorescence spectra were recorded after each addition.

The quantum-chemical calculations were carried out using the following program packages: Gaussian 09 [32] (optimization of the geometry of the ground and excited states) and NWChem 5.1 [33] (locally modified version with the addition of program code for carrying out ESS analysis [16] and calculation of the absorption spectra).

5-[4-(*N*,*N*-Dimethylamino)phenyl]-2-(4-pyridyl)-1,3-oxazole (1). A solution of 4-*N*,*N*-dimethylamino-ω-aminoacetophenone dihydrochloride (2.01 g, 8 mmol) and 4-pyridinecarboxylic acid (0.98 g, 8 mmol) in $POCl_3$ (30 ml) was heated at reflux for 1.5 h until HCl was no longer generated (tested on moist indicator paper). The reaction mixture was then poured onto ice (0.5 kg) and made weakly alkaline by adding powdered sodium carbonate. The precipitate formed was filtered off, washed with water until the wash water was neutral, and dried in air. The product was purified by chromatography on an alumina column at elevated temperature, close to the boiling point of the benzene eluent, and then recrystallized twice from water. The purity was monitored by thin-layer chromatography. Yield 1.43 g (67%). Yellow needles. Mp 238-237°C. ^{1}H NMR spectrum, δ, ppm (*J*, Hz): 8.73 (2H, d, *J* = 6.1, H-2,6-Py); 7.93 (2H, d, *J* = 6.1, H-3,5-Py); 7.68 (2H, d, *J* = 9.0, H-2,6 Ar); 7.66 (1H, s, H-4); 6.81 (2H, d, *J* = 9.0, H-3,5 Ar); 2.97 (6H, s, $N(CH_3)_2$). ^{13}C NMR spectrum, δ, ppm: 156.6, 153.1, 150.6 (CH); 133.6, 125.6 (CH); 121.5 (CH); 119.2 (CH); 114.4, 112.1 (CH); 39.8 ($N(CH_3)_2$). Found, %: C 72.55; H 5.69; N 15.83. $C_{16}H_{15}N_3O$. Calculated, %: C 72.43; H 5.70; N 15.84.

The authors express their sincere gratitude to Prof. N. A. Vodolazkaya (V. N. Karazin Kharkiv National University) for supplying samples of the different surfactants and participating in a discussion of these results and to Prof. Jerzy Błażejowski (Gdansk University, Poland) for cooperation in the measurement of the NMR spectra.

This work was carried out using the computer resources of the joint computer cluster of the "Institute of Single Crystals" and the Institute of Scintillation Materials, National Academy of Sciences of Ukraine, in conjunction with the Ukrainian national grid.

REFERENCES

1. Yu. A. Vladimirov and G. E. Dobretsov, *Fluorescence Analysis of Biological Membranes* [in Russian], Nauka, Moscow (1986), p. 9.
2. W. T. Mason (editor), *Fluorescent and Luminescent Probes for Biological Activity*, Academic Press, San Diego (1993), p. 17.
3. J. R. Lakowicz, *Principles of Fluorescence Spectroscopy*, 3rd ed., Springer, New York (2006), p. 63.
4. *Molecular Probes Handbook. A Guide to Fluorescent Probes and Labeling Technologies*, 11th ed., Molecular Probes® (2010), p. 1.
5. B. M. Krasovitskii and B. M. Bolotin, *Organic Luminophores* [in Russian], Khimiya, Moscow (1984), p. 71.
6. F. N. Hayes, B. S. Rogers, and D. G. Ott, *J. Am. Chem. Soc.*, **77**, 1850 (1955).
7. D. G. Ott, F. N. Hayes, and V. N. Kerr, *J. Am. Chem. Soc.*, **78**, 1941 (1956).
8. R. Yu. Il'yashenko, E. S. Roshchina, and A. O. Doroshenko, *Vestn. Kharkovsk. Nats. Univ.*, **932**, 9 (2010).
9. http://scifinder.cas.org.
10. https://www.reaxys.com.
11. A. D. Becke, *J. Chem. Phys.*, **98**, 5648 (1993).
12. D. E. Woon and T. H. Dunning, Jr., *J. Chem. Phys.*, **98**, 1358 (1993).
13. R. F. W. Bader, *Acc. Chem. Res.*, **18**, 9 (1985).
14. R. F. W. Bader, *Chem. Rev.*, **91**, 7314 (1991).
15. R. F. W. Bader, *J. Phys. Chem. A*, **102**, 7314 (1998).

16. A. V. Luzanov and O. A. Zhikol, *Int. J. Quantum Chem.*, **110**, 902 (2008).
17. E. Espinosa, E. Molins, and C. Lecomte, *Chem. Phys. Lett.*, **285**, 170 (1998).
18. A. V. Luzanov, *Usp. Khim.*, **64**, 2086 (1980).
19. W. Rettig, *Angew. Chem., Int. Ed. Engl.*, **25**, 971 (1986).
20. E. Lippert, W. Rettig, V. Bonacic-Koutecky, F. Heisel, and J. A. Miehe, *Adv. Chem. Phys.*, **68**, 1 (1987).
21. A. O. Doroshenko and V. G. Pivovarenko, *J. Photochem. Photobiol., A*, **156**, 55 (2003).
22. C. Reichardt, *Chem. Rev.*, **94**, 2319 (1994).
23. S. B. Savvin, R. K. Chernova, and S. N. Shtykov, *Surfactants* [in Russian], Nauka, Moscow (1991).
24. V. S. Bel'skii, *Izv. Akad. Nauk*, *Ser. Khim.*, 248 (2000) [*Russ. Chem. Bull.*, **49**, 251 (2000)].
25. N. O. Mchedlov-Petrosyan, L. P. Loginova, and V. N. Kleshchevnikova, *Zh. Fiz. Khim.*, **67**, 1649 (1993).
26. N. O. Mchedlov-Petrosyan, A. V. Plichko, and A. S. Shumakher, *Khim. Fiz.*, **15**, 105 (1996).
27. N. Schenfeld, *Ethylene Oxide Surfactants* [Russian translation], Khimiya, Moscow (1982), p. 331.
28. N. A. Vodolazkaya, P. V. Shakhova, and N. O. Mchedlov-Petrossyan, *Zh. Obshch. Khim.*, **79**, 1081 (2009).
29. A. A. Abramzon, *Surfactants: Properties and Applications* [in Russian], Khimiya, Leningrad (1981), p. 35.
30. W. H. Melhuish, *J. Res. Natl. Bur. Stand.*, *Sect. A*, **76A**, 547 (1972).
31. V. V. Aleksandrov, *Acidity of Nonaqueous Solutions* [in Russian], Vishcha Shkola, Kharkov (1981), p. 78.
32. M. J. Frisch, G. W. Trucks, H. B. Schlegel, G. E. Scuseria, M. A. Robb, J. R. Cheeseman, G. Scalmani, V. Barone, V. Mennucci, G. A. Petersson, H. Nakatsuji, M. Caricato, X. Li, H. P. Hratchian, A. F. Izmaylov, J. Bloino, G. Zheng, J. L. Sonnenberg, M. Hada, M. Ehara, K. Toyota, R. Fukuda, J. Hasegawa, M. Ishida, T. Nakajima, Y. Honda, O. Kitao, H. Nakai, T. Vreven, J. A. Montgomery, Jr., J. E. Peralta, F. Ogliaro, M. Bearpark, J. J. Heyd, E. Brothers, K. N. Kudin, V. N. Staroverov, T. Keith, R. Kobayashi, J. Normand, K. Raghavachari, A. Rendell, J. C. Burant, S. S. Iyengar, J. Tomasi, M. Cossi, N. Rega, J. M. Millam, M. Klene, J. E. Knox, J. B. Cross, V. Bakken, C. Adamo, J. Jaramillo, R. Gomperts, R. E. Stratmann, O. Yazyev, A. J. Austin, R. Cammi, C. Pomelli, J. W. Ochterski, R. L. Martin, K. Morokuma, V. G. Zakrzewski, G. A. Voth, P. Salvador, J. J. Dannenberg, S. Dapprich, A. D. Daniels, O. Farkas, J. B. Foresman, J. V. Ortiz, J. Cioslowski, and D. J. Fox, *Gaussian 09, B.01*, Gaussian Inc., Wallingford (2010).
33. E. J. Bylaska, W. A. de Jong, N. Govind, K. Kowalski, T. P. Straatsma, M. Valiev, D. Wang, E. Apra, T. L. Windus, J. Hammond, P. Nichols, S. Hirata, M. T. Hackler, Y. Zhao, P.-D. Fan, R. J. Harrison, M. Dupuis, D. M. A. Smith, J. Nieplocha, V. Tipparaju, M. Krishman, Q. Wu, T. Van Voorhis, A. A. Auer, M. Nooijen, E. Brown, G. Cisneros, G. I. Fann, H. Fruchtl, J. Garza, K. Hirao, R. Kendall, J. A. Nichols, K. Tsemekhman, K. Wolinski, J. Anchell, D. Bernholdt, P. Borowski, T. Clark, D. Clerc, H. Dachnel, M. Deegan, K. Dyall, D. Elwood, E. Glendening, M. Gutowski, A. Hess, J. Jaffe, B. Johnson, J. Ju, R. Kobayashi, R. Kutteh, Z. Lin, R. Littlefield, X. Long, B. Meng, T. Nakajima, S. Niu, L. Pollack, M. Rosing, G. Sandrone, M. Stave, H. Taylor, G. Thomas, J. van Lenthe, A. Wong, and Z. Zhang, *NWChem. A Computational Chemistry Package for Parallel Computers, Version 5.1*, Pacific Northwest National Laboratory, Richland, Washington (2007).